ID-1350

SPECTRUM RESPONSE OF EMBEDDED FIBER BRAGG GRATING SENSORS IN COMPLICATED STRAIN FIELD

Xiaoming Tao[a], Aping Zhang[a,b], DongxiaoYang[a,c] , and Hwa-Yaw Tam[b]

[a] *Institute of Textiles and Clothing, The Hong Kong Polytechnic University, HK*
[b] *Department of Electrical Engineering, The Hong Kong Polytechnic University, HK*
[c] *Department of Information and Electronic Engineering, Zhejiang University, PRC*

SUMMARY: This paper investigates the variations of reflection spectra of embedded fiber Bragg gratings sensor in composites brought by the complicated deformation conditions, namely, strain induced grating apodization and spectrum split. The geometric change of the fiber is considered together with the strain-induced permittivity perturbations in the fiber gratings. Due to strain induced birefringence characteristics, the fundamental mode in single mode fiber has been divided into LPx and LPy modes when discussing reflection spectra of FBG sensor in strain field. Numerical simulations have been presented based on the coupled mode theory.

KEYWORDS: embedded fiber Bragg grating sensor, reflection spectra, complicated strain, smart materials and structures

INTRODUCTION

Fiber Bragg grating (FBG) sensors have been embedded in smart materials and structures for monitoring or measuring their mechanical responses or temperature. In most of these applications, FBG sensors are applied to monitor or measure unidirectional strain. The optical responses of such fiber sensors can be analyzed in a simplified manner. However, with the rapid development of FBG sensors for different engineering applications, the embedded FBGs in composites are expected to work under complex deformations. The optical responses of such fiber sensors are complicated, and interpretation of experimental results is often difficult.

Reflective/transmission spectra of fiber Bragg gratings have been analyzed by using the coupled mode theory[1-5]. The coupling from forward to backward modes is determined as a phase-matching condition, namely the Bragg condition, which is related to the effective index and period of grating structure. Assuming that the FBG sensor is under a uniform axial stress, the changes in the effective index and period can be deduced from the strain-optic relationship and geometrical deformations. Resort to effective Pockel's constant to represent their combination effects, such strain induced shift of reflected peak is expressed as $\Delta \lambda_B = \lambda_B \cdot (1 - P_e) e_z$. In the case of FBG sensor embedded in the composites, residual stress and transversely load are inevitably introduced from the fabrication procedures and working environment. Apparently the fabrication induced residual stress or strain is random and

related to the composite microstructure and the control procedures. Hence the nonuniform axial strain may reconstruct the grating structure and lead to variations in the grating period, i.e. form the grating apodization. In some conditions the FBG sensor is under transverse loading, such as lateral impact etc. The effects of strain induced birefringence characteristics must be considered. Induced difference of propagation constants of LPx and LPy modes may result in split of reflection spectra.

This paper investigates these variations of reflection spectrum response of FBG sensors, which may be found in FBG sensor embedded composites. The fundamental mode in a single-mode fiber is divided into LPx and LPy modes when discussing reflection spectra of FBG sensor in a strain field. The scalar coupled mode theory will be extended to vector forms to include the strain induced anisotropic characteristics. Numerical examples have been presented based on the unified analysis of reflection spectra of FBG sensors in various strain field.

FIBER BRAGG GRATINGS IN A GENERAL STRAIN FIELD

Coupled mode theory is often used to analyze the reflection spectra of fiber Bragg gratings, where the reflected waves from the grating structure are described as the coupling from the forward modes to backward ones. If considering the reflection spectra of FBG sensors in a general strain field, then we should include both the permittivity perturbation formed with grating structure and that induced by the strain. The strain-induced optical impermeability perturbation $\Delta \mathbf{B}_{ij}$ can be expressed as

$$\Delta \mathbf{B}_{ij} = \mathbf{p}_{ijkl} \mathbf{e}_{kl}, \tag{1}$$

where $\mathbf{p}_{ijkl}$ and $\mathbf{e}_{kl}$ are the strain-optic tensor and the strain tensor, respectively. Differing from the UV irradiation, which normally confines its effect on the core, the strain affects the refractive index of both the core and cladding. From the relationship between the impermeability and the relative permittivity, $\mathrm{B}_{ij} = 1/\mathrm{å}_{ij}$, and the relationship between relative permittivity and refractive index, $\mathrm{å}_{ij} = \mathrm{n}_{ij}^2$, the strain-induced relative permittivity perturbations of an optical fiber with an effective index n_{eff} is

$$\Delta \mathbf{å}_{st} = -n_{eff}^4 \cdot \mathbf{p}_{ijkl} \mathbf{e}_{kl}. \tag{2}$$

Though linear birefringence characteristic is also concomitant with the side-exposure technology in FBG sensors, it can often be depressed[6, 7] and neglected in discussing the spectra of fiber gratings. Hence the refractive index perturbation by the UV irradiation can be

described as

$$\delta n_{gr} = \delta n_{dc} + \delta n_{ac} \cdot \cos[\frac{2\pi}{\Lambda} \cdot z + f(z)], \tag{3}$$

where δn_{dc} and δn_{ac} are the "dc" and "ac" index modulation component, Λ is the grating period, and $f(z)$ describes the grating chirps, respectively. With the help of identity matrix $\mathbf{I}$, the relative permittivity perturbation of fiber phase gratings in a strain field can be expressed as

$$\Delta\boldsymbol{\varepsilon}_r = \begin{cases} \Delta\boldsymbol{\varepsilon}_{st} + 2n_{eff} \cdot \delta n_{gr} \cdot \mathbf{I}, & \text{in the core} \\ \Delta\boldsymbol{\varepsilon}_{st}, & \text{in the cladding} \end{cases} \tag{4}$$

Under deformation, the UV induced index perturbation δn_{gr} is re-distributed within the fiber. Therefore the grating structure as expressed in Eqn.3 should be corrected with the displacement in strain field.

With the occurrence of strain-induced birefringence, it is necessary to extend scalar coupled mode equations to vector forms to include the strain induced anisotropic characteristics of the permittivity perturbations. Vectorial forms of coupled mode equations has been used to polarization analysis[8-9]. If a_j and b_j are denoted as the complex amplitude of forward and backward LP modes respectively, the coupled mode equations can be expressed as

$$\frac{da_j(z)}{dz} = i\sum_{k=1}^{2} \kappa_{jk}^{t} \cdot a_k(z) \exp[i(\beta_k - \beta_j)z] + i\sum_{k=1}^{2} \kappa_{jk}^{t} \cdot b_k(z) \exp[-i(\beta_k + \beta_j)z], \tag{5.a}$$

$$\frac{db_j(z)}{dz} = -i\sum_{k=1}^{2} \kappa_{jk}^{t} \cdot a_k(z) \exp[i(\beta_k + \beta_j)z] - i\sum_{k=1}^{2} \kappa_{jk}^{t} \cdot b_k(z) \exp[-i(\beta_k - \beta_j)z], \tag{5.b}$$

where

$$\kappa_{jk}^{t} = \frac{1}{4}\omega \cdot \varepsilon_0 \iint (\Delta\boldsymbol{\varepsilon}_r \mathbf{E}_k) \bullet \mathbf{E}_j^{*} dA\,. \tag{5.c}$$

and the electric modes $\mathbf{E}_j$ have been normalized. The axial coupling coefficient component has been neglected, since it is a much smaller term comparing to the transverse ones in single mode fiber.

Currently two standard approaches are used for numerically calculating the spectra of FBG sensor. The first is a direct integration of the coupled mode equations and the second is a

piecewise-uniform approach[4]. Since the strain induced permittivity perturbation may be random along the fiber embedded in a composites. The latter approach is difficult to implement. Improvement should also be made for the first approach to allow arbitrary input light with given polarization state. Coupled mode equations can be rewritten in vector operational forms as

$$\begin{Bmatrix} \mathbf{A}' \\ \mathbf{B}' \end{Bmatrix} = [\mathbf{T}] \cdot \begin{Bmatrix} \mathbf{A} \\ \mathbf{B} \end{Bmatrix} \tag{6}$$

where $\mathbf{A} = \{a_1, a_2\}^T$, $\mathbf{B} = \{b_1, b_2\}^T$, $[\mathbf{T}]$ is the corresponding matrix of coupling coefficients, and the prime denotes the first order derivative with respect to the axial coordinate z. Its corresponding discrete form is

$$\begin{Bmatrix} \mathbf{A}^n \\ \mathbf{B}^n \end{Bmatrix} = [\tilde{\mathbf{T}}] \cdot \begin{Bmatrix} \mathbf{A}^0 \\ \mathbf{B}^0 \end{Bmatrix} \tag{7}$$

where

$$[\tilde{\mathbf{T}}] = [\tilde{\mathbf{T}}^{n-1}] \cdot [\tilde{\mathbf{T}}^{n-2}] \cdots [\tilde{\mathbf{T}}^{1}] \cdot [\tilde{\mathbf{T}}^{0}], \quad \text{and} \quad [\tilde{\mathbf{T}}^{k}] = [\mathbf{I}] + [\mathbf{T}^{k}] \cdot dz^{k}.$$

From the boundary condition $\mathbf{A}^0 = \{a_1^0, a_2^0\}^T$, $\mathbf{B}^n = 0$, we can obtain the reflected optical wave components $\mathbf{B}^0$ from Eqn.7 as

$$\mathbf{B}^0 = \frac{1}{\tilde{T}_{33} \cdot \tilde{T}_{44} - \tilde{T}_{43} \cdot \tilde{T}_{34}} \cdot \begin{Bmatrix} \hat{a}_1 \cdot \tilde{T}_{44} - \hat{a}_2 \cdot \tilde{T}_{34} \\ \hat{a}_2 \cdot T_{33} - \hat{a}_2 \cdot \tilde{T}_{43} \end{Bmatrix}, \tag{8}$$

where

$$\hat{a}_1 = -1 \cdot (a_1^0 \cdot \tilde{T}_{31} + a_2^0 \cdot \tilde{T}_{32}), \quad \text{and} \quad \hat{a}_2 = -1 \cdot (a_1^0 \cdot \tilde{T}_{41} + a_2^0 \cdot \tilde{T}_{42}).$$

If the optical power is taken as its periodic average[10], the reflectivity R can be defined by $\mathbf{A}^0$ and $\mathbf{B}^0$ as

$$R = \frac{|b_1^0|^2 + |b_2^0|^2}{|a_1^0|^2 + |a_2^0|^2}. \tag{9}$$

Then a unified analysis of the reflection spectra of FBG sensor in an arbitrary strain field can be applied. Since the residual and transverse stresses are inevitable in the composites, as

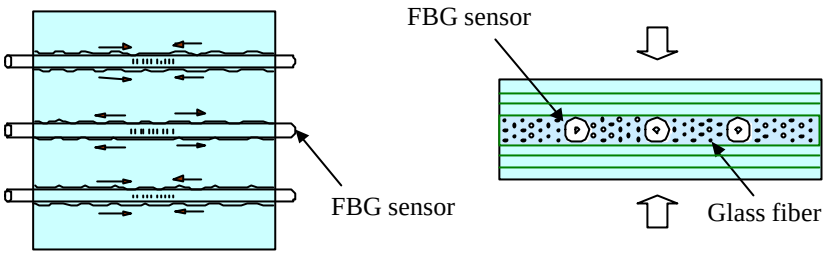

Fig.1 Composite embedded with FBG sensors. (a) Random Residual Stress on FBG Sensor. (b) Transversely Loading on FBG sensor.

shown in Fig.1, we will present an analysis of spectrum response together with numerical simulations.

STRAIN INDUCED GRATING APODIZATION

It is known that the Bragg condition of FBG sensor is related to both effective index and period of FBG sensor. Linear relationship between strain and induced shift of Bragg wavelength can be deduced if the axial strain is assumed to be uniform along the FBG sensor. However the residual strain distribution in composites is often random and nonuniform, it is necessary to study the effects of the nonuniform axial strain on the spectrum response of FBG sensor.

If the origin of a coordinate system is located at input end of the gratings, and assume the strain distribution along the length of FBG is described by polynomial approximations as

$$e_z(z) = \sum_{i=0}^{k} e_{(i)} \cdot (\frac{z}{L})^i \ , \tag{10}$$

where L is the length of the gratings. Let $\Lambda_{[j]}$ represent the jth period of the grating, which can be expressed by displacement obtained by integrating Eqn.10

$$\Lambda_{[j]} = \Lambda_0 \left\{ 1 + \sum_{i=0}^{k} \frac{e_{(i)}}{(i+1) \cdot L^i} \cdot \Lambda_0^i [\, j^{i+1} - (j-1)^{i+1}] \right\}. \tag{11}$$

Apparently this grating structure has changed from a uniform into a chirp one. Assume such strain is resulted from a nonuniform and unidirectional stress. Relational expression between the effective index perturbation and the axial strain can be obtained from the optic-strain relationship as

$$\Delta n_{eff}(z) = -(n_{eff}^3 / 2)[(P_{12} - vP_{11} - vP_{12}) e_z(z)] \, , \tag{12}$$

Table I. Parameters of Single Mode Fiber

Radius of Core	R_{co}	4.25 μm
Radius of Cladding	R_{cl}	62.5 μm
Refractive index of Core	N_{co}	1.466
Refractive index of Cladding	N_{cl}	1.462
Strain-optic coefficient	P_{11}	0.113
Strain-optic coefficient	P_{12}	0.252

where n_{eff} and ν are the effective refractive index and the Poisson's ratio, respectively.

Considering the case of a uniform strain field, the change of period can be obtained from Eqn.11 as $\Delta\Lambda = e_z \cdot \Lambda_0$, and the change of effective index can be obtained from Eqn.12 as $\Delta n_{eff} = -(n_{eff}^3/2)(P_{12} - \nu P_{11} - \nu P_{12}) \cdot e_z$. Since the relative shift of Bragg wavelength λ_B is $\Delta\lambda_B/\lambda_B = \Delta\Lambda/\Lambda + \Delta n_{eff}/n_{eff}$, the relation between the shift of Bragg wavelength and the axial strain then is

$$\Delta\lambda_B = \lambda_B \cdot (1 - P_e) e_z \qquad (13)$$

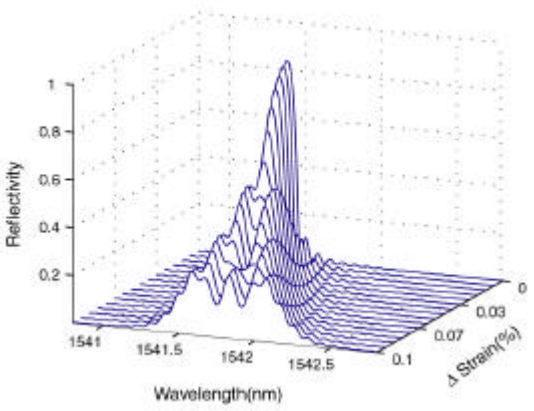

Fig.2 Nonuniform strain induced grating chirp. The modulation of "dc" and "ac" component of original grating is 2.0e-4 and 1.0e-4, respetively.

where the effective Pockel's constant $P_e = n_{eff}^2 \cdot [P_{12} - \nu(P_{11} + P_{12})]/2$. In the case of a nonuniform strain field, such relation is not valid any more. As normally a FBG is short, the linear approximation can be used to represent the nonuniform strain as $e(z) = e(0) + \Delta e \cdot z/L$, where the strain difference is $\Delta e = e(L) - e(0)$. Numerical examples of reflection spectra are presented in Fig.2, where the parameters of a single mode fiber are listed in Table 1. The strain difference Δe varies from 0.0 to 0.1 percent.

SPECTRUM SPLIT

Spectrum split indicates the phenomenon that a single-peak spectrum becomes double-peak one under special conditions. If an embedded FBG sensor is under a transversely loading, the anisotropic strain field will induce an anisotropic permittivity perturbation, namely linear birefringence. According to the Bragg conditions, the spectrum split is expected as a result of different propagation constants of two LP modes.

In order to simplify the discussion of the effects of transverse strain field, we approximate the external loading on FBG sensor as a line force along the axial direction. Based on a plane stress assumption, the stresses in the core are $\sigma_x = f/\pi R_{cl}$, $\sigma_y = -3f/\pi R_{cl}$, where f is

the line force, y axis is selected as the loading direction. Based on previous analysis of FBG sensor in strain field, numerical simulations of reflection spectra in such transverse strain are presented in Fig.3, where the parameters in Table 1 is still used in calculations. Young's modulus of silica optical fiber E is $72.5GPa$, poisson's ratio v is 0.16. The loading line force varies from 0.0 to 3.0KN/m, and the orientation angles of input linear polarized light in diagrams A to C correspond to 0.0, $\pi/6$, $\pi/4$, respectively.

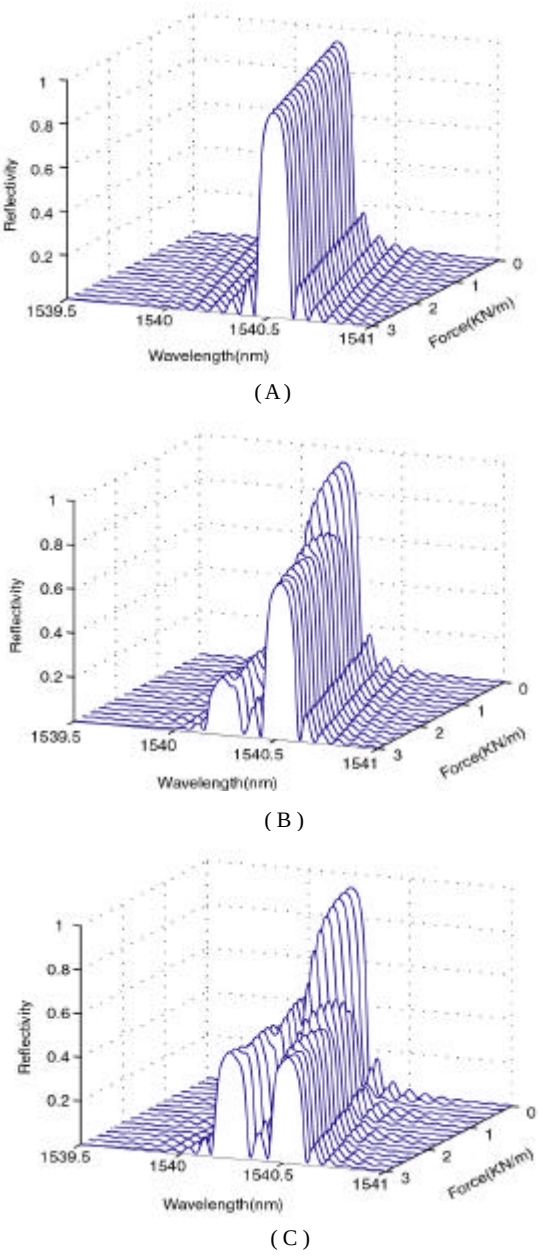

Fig.3 Reflection spectra of FBG sensor under transverse strain effects. (A) Orientation angle of input linear polarized light is 0.0; (B) Orientation angle is $\pi/6$; (C) Orientation angle is $\pi/4$.

DISCUSSIONS

Numerical examples of spectrum response of FBG sensor with the effects of nonuniform axial strain have been presented on Fig.2, and reflection spectra of FBG sensor under transverse strain field have been presented in Fig.3. Complexity of reflection spectrum is found increased in such strain field.

In the case of nonuniform longitude strain field, Eqn.12 shows that the effective index linearly varies along the axial strain distribution. If the first order approximation is used to represent the nonuniform strain distribution, the linear sensitivity characteristic of FBG sensor is still held. The broadening of FBG bandwidth can be regarded as the increment of FBG wavelength. Then the strain difference can be deduced from the increment of reflection bandwidth Δl_{RB} as $\Delta e = \Delta l_{RB} / l_B (1 - P_e)$. A much simpler treatment is proposed to adopt the middle of spectrum bandwith as the valid Bragg wavelength. Thus the average strain along the grating length is derived from that for the normal gratings.

In the case of FBG sensor in a transverse strain field, as shown in Fig.3, the input polarization states have effects on the reflection spectra of FBG sensor. The functionary components of input polarization states are the amplitude of LPx and LPy components, which indicate its carried optical power. If input only LPx (or LPy) component, we can observe a shift of spectrum. The spectrum will be splitted if both LPx and LPy component have been inputted.

Hence it is necessary to control the input polarization states to obtain a stable reflection spectrum in the case of FBG sensor in a transverse strain field. If the magnitude of reflection split $\Delta \lambda_B$ can be observed, the strain difference Δe_{x-y} can be inversely deduced as

$$\Delta e_{x-y} = \frac{2}{n_{eff}^2 (p_{12} - p_{11})} \cdot \frac{\Delta \lambda_B}{\lambda_B}. \tag{14}$$

In some special cases, the relation between transverse strains can be known from mechanical analysis. Therefore the transverse strain components can be obtained from further deduction from Eqn.14. Apparently it is important to distinguish the spectrum split induced from transverse strain from nonuniform strain apodization. The spectrum broadening and splitting by nonuniform strain is independent of the initial polarization states of the input light, in the contrast of those caused by the transverse strain induced birefringence.

CONCLUSIONS

This paper has investigated the variations of reflection spectra of embedded FBG sensor in composites in the complicated strain fields. The geometric changes of the fiber and the strain-induced birefringence have been found to have significant effects on the reflection spectra of FBG sensor. Numerical examples of strain induced apodization and transverse strain induced spectrum split have been presented based on the coupled mode theory.

REFERENCES

1. Hermann A. Haus and Weiping Huang, Coupled-Mode Theory, Proceeding of The IEEE, Vol.79, No.10, 1991, pp. 1505-1518.
2. W.P. Huang, Coupled-mode theory for optical wave-guides – An overview, J.Optical Soc.Am.A, Image Science and Vision, Vol.11, pp.963-983, 1994.
3. Martin McCall, On the Application of Coupled Mode Theory for Modeling Fiber Bragg Gratings, Journal of Lightwave Technology, Vol.18, No.2, 2000, pp.236-242.
4. T.Erdogan, Fiber Grating Spectra, Journal of Lightwave Technology, vol.15, No.8, 1997, pp.1277-1294.
5. S.M. Norton, T.Erdogan, G.M. Morris, Coupled-mode theory of resonant-grating filters, J.Optical Soc.Am.A, Image Science and Vision, Vol.14, Iss.3, pp.629-639, 1997.
6. T.Erdogan and V.Mizrahi, Characterization of UV induced birefringence in photosensitive Ge-doped silica optical fibers, J.Opt.Soc.Am.B., Vol.11, No. 10, 1994, pp.2100-2105.
7. Ashish M.Vengsarkar, Qian Zhong, Dary Inniss, W.A.Reed, Paul J.Lemaire, and S.G.Losinski, Birefringence reducation in sider-written photoinduced fiber devices by a dual-exposure method, Optics Letter, Vol.19, No.16, 1994, pp.1260-1262.
8. J.I. Sakai, T.Kimura, Polarization Behavior in Multiply Perturbed Single-Mode Fibers, IEEE J.Quantum Electron, Vol.QE-18, No.1, pp.59-65, 1981.
9. J.I.Sakai, T.Kimura, Birefringence and Polarization Characteristics of Single Mode Fibers under Elastic Deformations, J.Quantum Electron, Vol.QE-17: No.6, pp.1041-1051, 1981.
10. Yu Yunqiang, A Concise Course on the Electrodynamics, Peking University Press, 1999.